The work at this laboratory[19] has indicated that correlation between experimental and calculated γ-ray distributions in $(n,n'\gamma)$ reactions can lead to the determination of nuclear level spin and parity. The inclusion of width-fluctuation effects in the calculation of γ-ray cross sections will improve the reliability of this technique for the level spin and parity assignments.

[19] S. C. Mathur, P. S. Buchanan, and I. L. Morgan, Nucl. Phys. **81**, 468 (1966).

ACKNOWLEDGMENTS

The authors wish to express their appreciation to Dr. P. A. Moldauer for helpful communications and for the use of his computer program NEARREX. It is a pleasure to thank Professor E. Sheldon for making his computer program MANDY available to us and permitting subsequent modifications to it. We are indebted to Professor E. L. Hudspeth for his interest in this research and for making available the CDC-6600 computer facility at the University of Texas.

PHYSICAL REVIEW VOLUME 160, NUMBER 4 20 AUGUST 1967

Breakup of O^{16} into Be^8+Be^8†

P. CHEVALLIER AND F. SCHEIBLING
Institut de Recherches Nucléaires, Strasbourg-Cronenbourg, France

AND

G. GOLDRING, I. PLESSER, AND M. W. SACHS*
The Weizmann Institute of Science, Rehovoth, Israel

(Received 27 January 1967)

The reaction $C^{12}+\alpha \rightarrow Be^8+Be^8$ was studied in the range of α energy 11.85 MeV$\leq E_{\alpha\ \mathrm{in}} \leq$19.4 MeV. The Be^8 nuclei were detected by a suitable counter system registering the α-particle decay products. The cross section for this reaction was found to be quite large. A number of resonances were identified, and their spins and parities were determined by angular-distribution measurements. There is an indication of a rotational-band pattern of some of the levels.

INTRODUCTION

A FEATURE of O^{16} which has been studied up to now by elastic or inelastic α scattering is its large α strength in the region of excitation around 20 MeV.[1,2] There is, however, a serious drawback in this direct approach in that the very high level density in this region tends to obscure most structure details. A more satisfactory procedure from this point of view is to study the breakup of O^{16} into two Be^8 nuclei which is also closely linked to the α-particle structure of O^{16}. In this reaction the number of possible angular momenta is severely reduced both by the symmetry of the configuration—confining the values of J^π to 0^+, 2^+, $4^+\cdots$—and by the limitations imposed by the momenta of the emitted Be^8 nuclei.

In the present work the reaction $C^{12}+\alpha \rightarrow Be^8+Be^8$ was studied within the energy range

$$11.85\ \mathrm{MeV} \leqslant E_{\alpha\ \mathrm{in}} \leqslant 19.4\ \mathrm{MeV}.$$

The excitation function at 90° c.m. was determined in

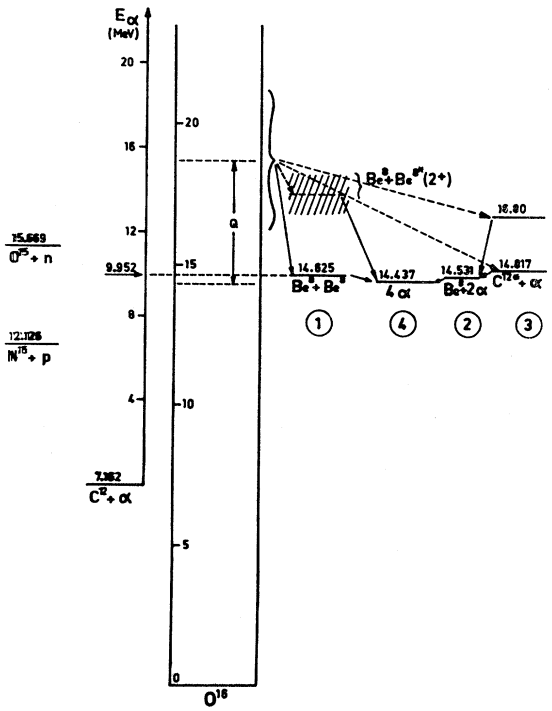

FIG. 1. Schematic diagram of various decay modes of excited O^{16} into four α's.

† A preliminary report on this work has been given at the Symposium on Recent Progress in Nuclear Physics with Tandems, Heidelberg, July, 1966.

* NATO fellow during 1965. Present address: Nuclear Structure Laboratories, Yale University, New Haven, Connecticut.

[1] E. B. Carter, G. E. Mitchel, and R. H. Davis, Phys. Rev. **133**, B1421 (1964).

[2] G. E. Mitchell, E. B. Carter, and R. H. Davis, Phys. Rev. **133**, B1434 (1964).

detail and the angular distribution of the emitted Be^8 was measured at several energies.

GEOMETRY OF EXPERIMENT

In the experiment here described the O^{16} nuclei were produced with an excitation energy of 16–20 MeV. In this range of excitation there are several distinct modes of decay into four α particles. The most important of these are the following decay chains:

1. $O^{16} \rightarrow Be^8 + Be^8$
   $Be^8 \rightarrow 2\alpha$
   $Be^8 \rightarrow 2\alpha$
2. $O^{16} \rightarrow Be^8 + 2\alpha$
   $Be^8 \rightarrow 2\alpha$
3. $O^{16} \rightarrow C^{12*}(0^+;\ 7.66\ \text{MeV}) + \alpha$(and higher states)
   $C^{12*} \rightarrow Be^8 + \alpha$
   $Be^8 \rightarrow 2\alpha$
4. $O^{16} \rightarrow 4\alpha$.

The energetics of these decay modes are indicated in Fig. 1. The different decay modes can be distinguished by their kinematic characteristics. These are shown schematically in Fig. 2 together with the sum of the energy of two α's in the O^{16} system. The $Be^8 + Be^8$ decay is seen to be unique in that it has a line spectrum in this system. In the laboratory system this is transformed

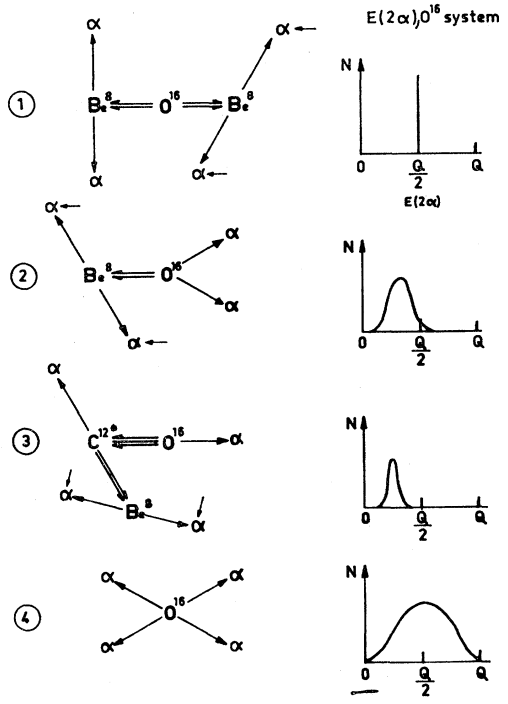

FIG. 2. Details of the successive steps of the decay modes indicated in Fig. 1. On the right-hand side is shown the spectrum of the sum of the energies of two α's (indicated by arrows) in the O^{16} system, i.e., the c.m. system for $\alpha + C^{12}$. Q is the energy available to four free α's, as shown in Fig. 1.

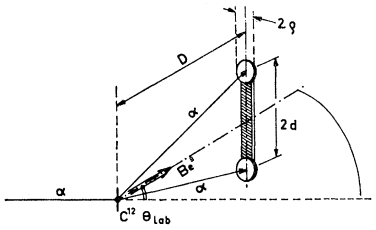

FIG. 3. Schematic drawing of counter arrangement. $2d = 1.8$ cm; $D = 5-9$ cm, depending on $E_{\alpha\,\text{in}}$; $2\rho = 0.8$ cm.

into a spectrum of well determined shape which can serve as an unambiguous signature for this particular process.

DESCRIPTION OF EXPERIMENT

Carbon foils of about 100 μg/cm^2 were bombarded by α's from a tandem Van de Graaff.[3] Be^8 nuclei emerging from the target were detected through their breakup into two α's by two junction counters of 50 mm^2 area situated as shown in Fig. 3.[4] The counters are in a plane perpendicular to the reaction plane $\alpha + C^{12} \rightarrow Be^8 + Be^8$ and they are positioned symmetrically with respect to this plane. The counting efficiency depends critically on the geometric parameters d and D. This is demonstrated in Fig. 4, which shows in detail the kinematics of the four α's and how the cone of α's emerging from one

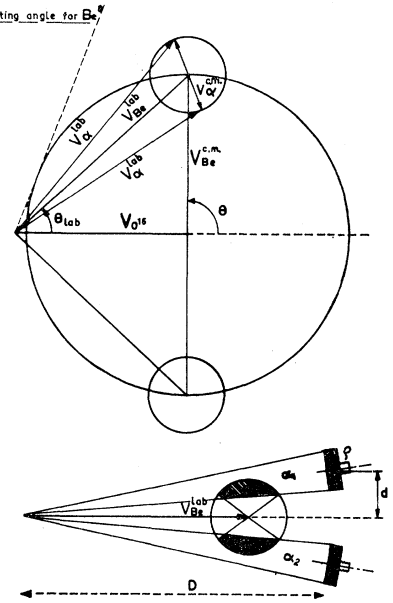

FIG. 4. Kinematics of α's in the reaction: $\alpha + C^{12} \rightarrow Be^8 + Be^8$, $Be^8 \rightarrow 2\alpha$; and detection efficiency for a pair of α's emerging from one Be^8.

[3] In the initial stages this experiment was conducted at the Daniel Heineman Accelerator Laboratory in Rehovoth, Israel, and the final measurements were carried out at the Max Planck Institut für Kernphysik in Heidelberg, Germany.

[4] A similar arrangement is described by Ronald E. Brown, J. S. Blair, D. Bodansky, N. Cue, and C. D. Kavaloski, Phys. Rev. **138**, B1394 (1965).

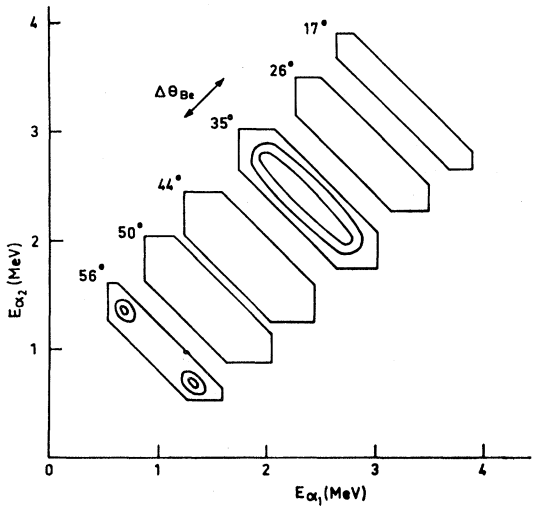

FIG. 5. Limits of the α energies for several lab angles at $E_{\alpha\ \mathrm{in}}=14.52$ MeV. For $\theta_{\mathrm{lab}}=35°$ and 56° the energy distribution is indicated in some detail.

Be^8 is viewed in the lab. It is evident that only a fraction of this cone is seen by the counters, the fraction depending strongly on the ratio $V_\alpha^{\mathrm{c.m.}}/V_{\mathrm{Be}}^{\mathrm{lab}}$ and therefore (for fixed d, D) on θ_{lab}. The values of d,D were chosen so as to yield maximum efficiency on the average. As a general indication we give the efficiency for the measurement at $E_{\alpha\ \mathrm{in}}=14.525$ MeV; $\theta=90°$ c.m. In that case the parameters d, D were $d=0.9$ cm, $D=7.0$ cm, and the efficiency was $\eta=2.91\times10^{-4}$ per O^{16} breakup.

Figure 5 shows the computed limits of α energies for α's from $O^{16}\rightarrow Be^8+Be^8$ (both Be^8 in ground state), $Be^8\rightarrow 2\alpha$, for several angles θ_{lab} in a particular case. At two angles the energy distribution is indicated in some detail.

Counts were recorded and the pulse heights analyzed in a two-dimensional multichannel analyzer. The counting logic is shown in Fig. 6. Two typical spectra are shown in Fig. 7.

The two-dimensional energy distributions of the coincidence counts were found in all cases to conform to the computed distributions. Figure 8 shows the density of counts for $\theta_{\mathrm{lab}}=35°$; $\theta_{\mathrm{lab}}=56°$, and $E_{\alpha\ \mathrm{in}}=14.52$ MeV, and may be compared with the computed distributions for these cases are shown in Fig. 5.

The identification of the Be^8+Be^8 events is grately facilitated by the fact that this is the dominant process in the relevant energy range of the two α's. In many cases the Be^8+Be^8 process was sufficiently well defined by the (one-dimensional) spectrum of the sum of the two energies. Several sum spectra of this type are shown in Fig. 9.

As a further check on this method of identification some measurements were carried out in an unfavorable case of low bombarding energy and low counting rate with an additional counter which accepted the α's from the conjugate Be^8. The results of these measurements were entirely consistent with those obtained in the usual way.

Other events identified in the sum spectra are inelastic scattering to the 0^+ level of C^{12} at 7.66 MeV (decay mode No. 3 in Figs. 1 and 2) and at high bombarding energies decay into Be^8+Be^{8*} with one Be^8 in the first excited 2^+ state.

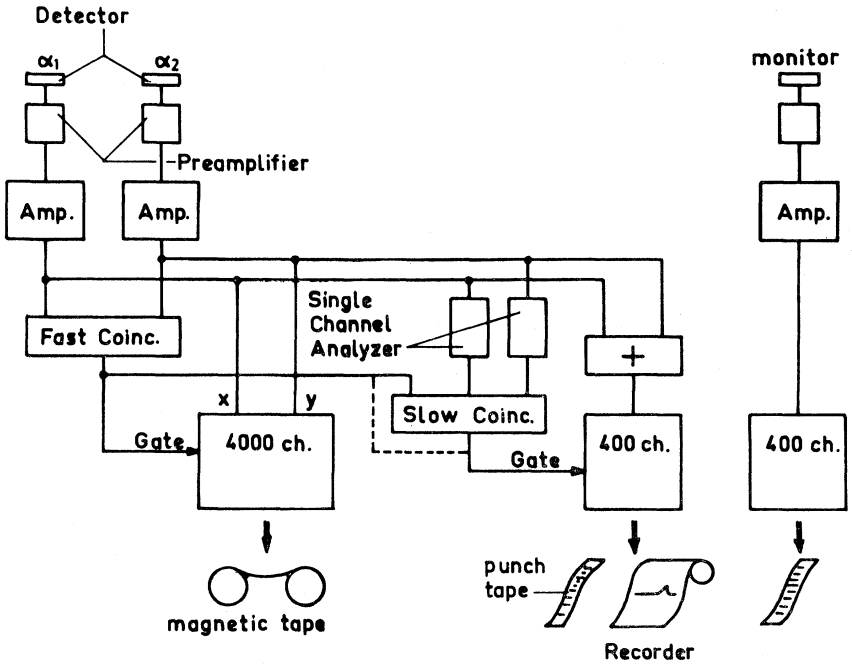

FIG. 6. Schematics of counting logic. The monitor was a fixed counter, at $\theta_{\mathrm{lab}}=90°$, mainly used for normalization in the angular-distribution measurements.

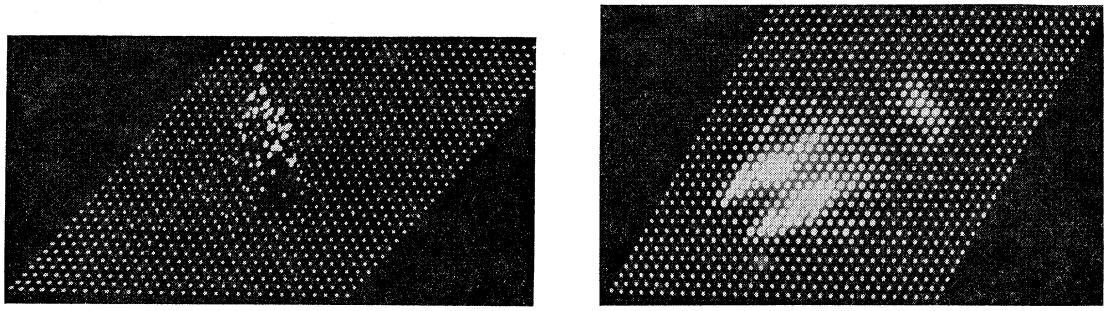

(a) (b)

FIG. 7. Two-dimensional spectra of the energies of the two α's. (a) A typical large-angle spectrum is shown in a "three-dimensional" display. Virtually all counts registered in this case correspond to $O^{16} \rightarrow Be^8+Be^8$ decays. (b) A typical "small-angle" spectrum shown in an intensity-modulation display. The α pairs from Be^8+Be^8 decays appear in this spectrum as the head of the little man.

RESULTS

The excitation function for the Be^8+Be^8 (both in ground state) decay was measured for α bombarding energies from 11.85 to 19.14 MeV at the Be^8 c.m. angle $\theta=90°$. The measured excitation function is shown in Fig. 10.

Angular-distribution measurements were carried out at several energies, in particular in regions of suspected resonances. All these measurements are summed up in Fig. 11.

If the excitation function is generated by a number of individual resonances, the angular distributions should be of the form

$$W(\theta)=\left|\sum_{L=0}^{L\max}\rho_L e^{i\varphi_L}P_L(\cos\theta)\right|^2, \quad \varphi_0=0$$

where $L_{\max}$ is not larger than the highest allowed L value.

We have therefore attempted to fit the measured angular distributions with functions of this form.

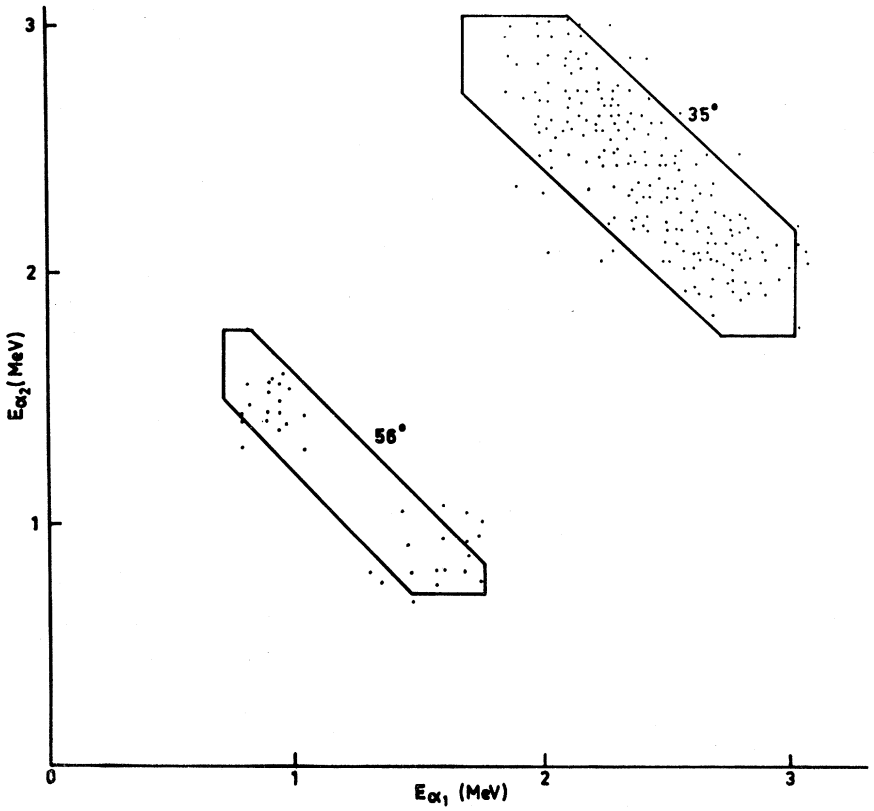

FIG. 8. Density of coincidence counts in the $E_{\alpha 1}$, $E_{\alpha 2}$ plane for $\theta_{lab}=35°$, $\theta_{lab}=56°$, and $E_{\alpha\,in}=14.52$ MeV. (1 point =1 coincidence.)

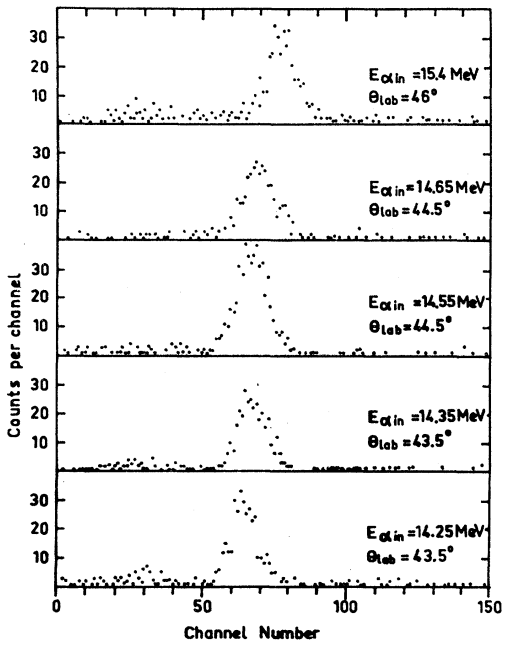

FIG. 9. Sum spectra at $\theta\sim 90°$ c.m.

One finds in such a fitting procedure that the parameters ρ_L, φ_L are defined in a unique manner for $L=L_{\max}$, but for $L<L_{\max}$ there are usually two solutions (for $L_{\max}=4$) or more (for $L_{\max}>4$). The various solutions all correspond to *one* angular distribution and one can distinguish among them only by considerations of continuity as a function of energy.

Table I gives the values of ρ_L, φ_L corresponding to the distributions shown in Fig. 11. For $L_{\max}=4$ the two solutions (for $L=0$, 2) are given. For $E_{\alpha\,\text{in}}=16.25$ MeV, $L_{\max}=6$, only one solution is given as the main point we wish to make in this case is that the $L=6$ component is essential for a good fit. This can be seen in the two fits shown in Fig. 12 for $E_{\alpha\,\text{in}}=16.25$ MeV, with $L_{\max}=6$ and $L_{\max}=4$, respectively.

DISCUSSION

The most striking feature of the excitation function is the uniformly large value of the cross section; it is of the same order of magnitude as the $N^{15}+p$ decay mode and only about ten times weaker than the quite strong inelastic α scattering.

Some of the peaks in the excitation function can definitely be established as resonances by the correlation of various reaction channels; the sharp feature at $E_{\alpha\,\text{in}}=14.50$ MeV is found in Be^8+Be^8, $N^{15}+p_0$, $C^{12}+\alpha_0$, $C^{12}+\alpha_1$ as shown in the enlarged drawing of this part of the excitation function in Fig. 10.

The measured width of this feature is ~ 20 keV, which is the estimated experimental energy spread. The true width of this level is therefore extremely small: $\Gamma \lesssim 20$ keV.

The two peaks at $E_{\alpha\,\text{in}}=13.05$ MeV and $E_{\alpha\,\text{in}}=13.35$ MeV are also found in $O^{15}+n_0$.[5]

The J^π values of the various resonances can be established from the angular distributions with varying degrees of certainty. For the resonances at 13.05 and 13.35 MeV, J^π is established in a unique manner as 2^+. From the behavior of the $L=0$ component in this region there is also a vague indication of a broad $L=0$ state in the neighborhood of 13 MeV. The J^π value for the resonance at 14.50 MeV can be determined from the

[5] S. S. Hanna, Symposium on Recent Progress in Nuclear Physics with Tandems. Heidelberg, July, 1966 (unpublished).

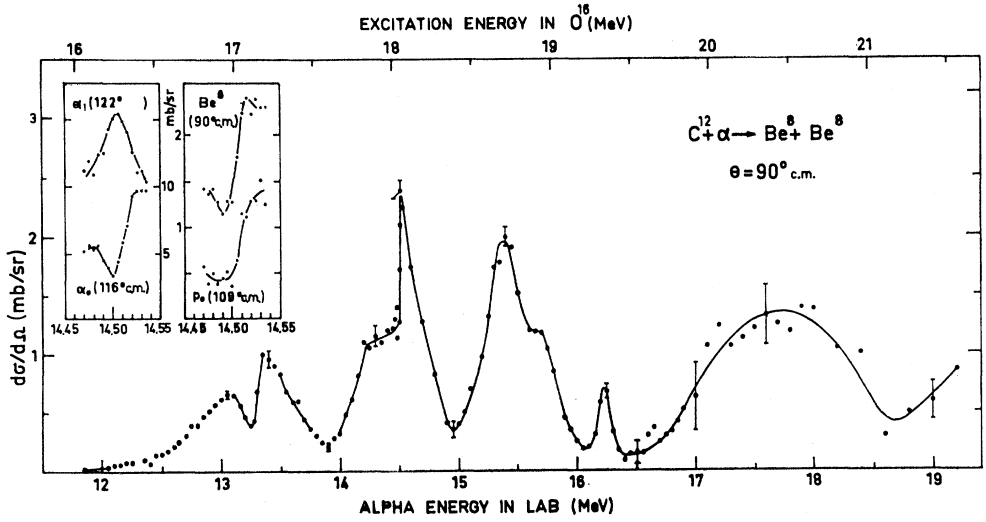

FIG. 10. The measured excitation function for the reaction $C^{12}+\alpha \rightarrow Be^8+Be^8$ at 90 c.m. angle. The classical limits for the various angular momenta [for $R(Be^8)=2.6$ F] are, respectively, 15.6, 18.5, and 23.4 MeV in O^{16}. The enlarged sections show details of the excitation in the neighborhood of 14.50 MeV for the Be^8+Be^8 channel as well as for other channels as indicated. The α_0, α_1, and p_0 data in the insert were taken with a monitor counter situated at 97° lab angle.

TABLE I. The parameters ρ_L, φ_L derived from a best fit to each angular distribution of the form

$$w(\theta)=\left|\sum_{L=0}^{L_{\max}}\rho_L e^{i\varphi_L}P_L(\cos\theta)\right|^2(\mu\text{b/sr}),\ \varphi_0=0.$$

For $L_{\max}=4$ the two possible solutions are given. The given values for ρ_L are actually the values of $\rho_L/(2L+1)^{1/2}$. $\varphi_0=0$ throughout.

E_α in (MeV)	$L_{\max}$	χ^2/N	$\sum\rho^2$	ρ_4	Solution $\rho_0<\rho_2$ ρ_0	φ_4	φ_2	φ_2	Solution $\rho_0>\rho_2$ ρ_2	ρ_0	φ_4	φ_2
12.700	2	1.88	266		11.6	11.5		123°				
13.050	2	6.52	580		20.4	12.8		117°				
13.350	2	5.02	892		27.6	11.3		107°				
13.550	2	4.52	795		23.8	14.8		117°				
14.1	4	1.55	1687	26.2	31.2	5.2	135°	80°	18.7	25.5	75°	62°
14.2	4	2.41	1237	26.0	23.0	5.7	136°	217°	4.2	23.3	80°	54°
14.3	4	1.37	1195	24.2	24.6	1.4	45°	− 43°	9.1	23.0	63°	− 23°
14.4	4	2.36	600	16.0	18.0	4.2	8°	131°	12.9	13.3	50°	− 90°
14.475	4	0.80	692	11.7	20.5	11.7	38°	149°	10.7	21.0	14°	−120°
14.490	4	1.30	750	13.2	20.6	12.3	56°	146°	6.7	23.0	34°	126°
14.505	4	0.95	1262	23.8	22.2	14.3	67°	164°	6.3	25.6	57°	172°
14.520	4	2.53	1154	22.3	20.2	15.7	49°	164°	9.2	23.9	46°	203°
14.525	4	1.04	1047	21.1	18.3	16.4	53°	164°	9.3	22.7	49°	185°
14.535	4	3.57	992	19.4	20.3	14.3	51°	165°	8.4	23.3	45°	210°
15.250	4	1.35	2690	31.3	40.0	10.4	170°	257°	9.6	40.2	75°	− 1°
15.400	4	2.54	1500	22.5	29.2	11.8	137°	244°	9.3	30.1	79°	− 71°
15.550	4	0.84	1281	26.2	23.1	7.9	129°	225°	2.7	24.3	81°	− 56°
15.700	4	1.95	1167	26.3	20.6	7.2	93°	180°	0.6	21.8	72°	172°
					ρ_6	ρ_4	ρ_2	ρ_0	φ_6	φ_4	φ_2	φ_0
16.250	6	0.98	816		16.7	18.7	13.0	3.8	− 55°	90°	169°	0

behavior of the parameters ρ_L in this region. The relevant ρ_L are shown in Fig. 13. It is quite obvious that ρ_4 is the only one which exhibits the characteristic "jump" at the resonance energy and the J^π value of this level is established in this way as 4^+.

The level at 16.25 MeV is established as 6^+ because the angular distribution at this point definitely indicates a substantial P_6 component, whereas at both lower

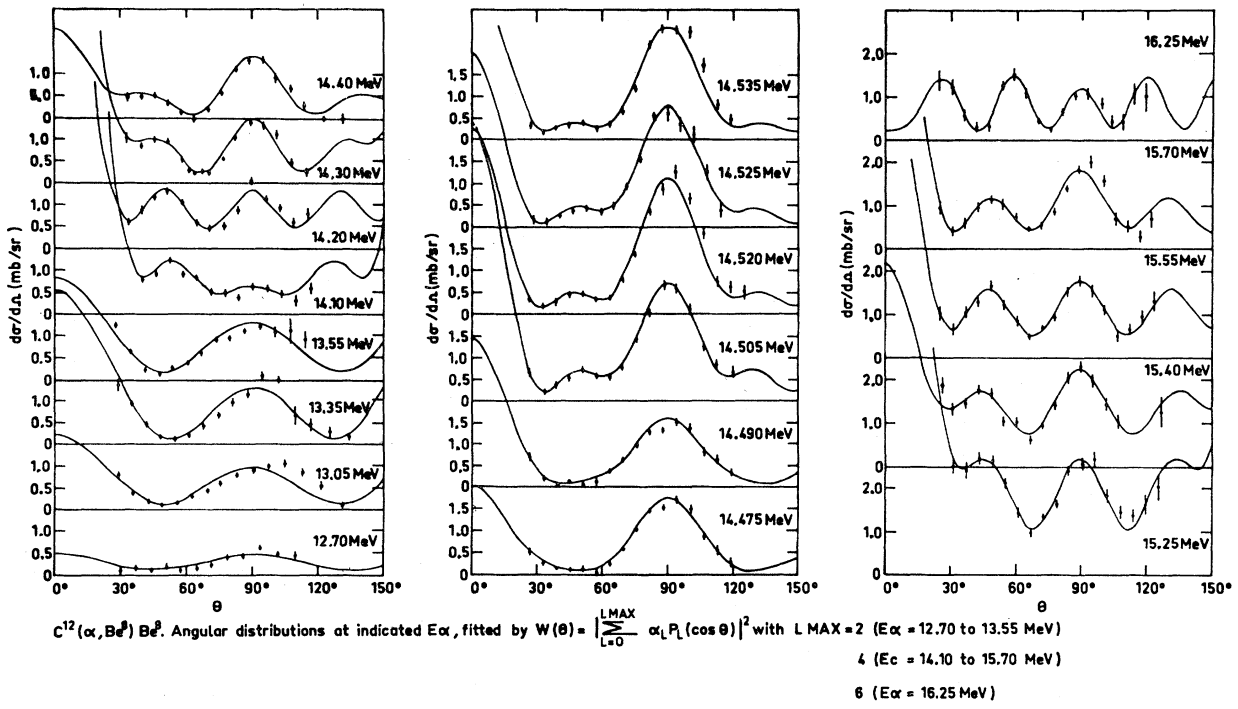

FIG. 11. Angular distribution measurements for the Be^8's, shown in the c.m. system. The solid line corresponds to the best fit obtained by a distribution of the type

$$w(\theta)=\left|\sum_{L=0}^{L_{\max}}\rho_L e^{i\varphi_L}P_L(\cos\theta)\right|^2;$$

$\varphi_0=0$. The parameters ρ_L, φ_L are given in Table I.

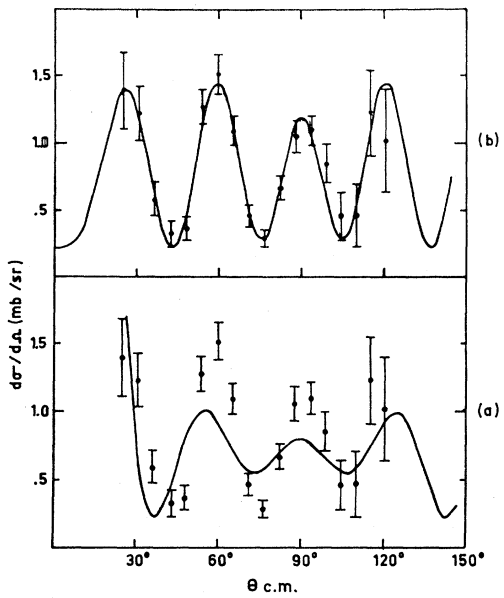

FIG. 12. Best fit to the 16.25-MeV angular distribution. (a) $L_{max}=4$; (b) $L_{max}=6$.

and higher energies (in this case with much less statistical significance) there is no indication of any $L=6$ angular momentum, and indeed this energy is well below the classical limit for $L=6$.

The complexity of the excitation function makes it difficult to single out and identify other resonances. Some tentative assignments have, however, been made and these are listed (in parentheses) in Table II together with the other more definite assignments.

The values of Γ in Table II are given on the basis of fairly crude one-level fits to the resonances and are therefore only rough estimates of the true parameters. The values Γ_{Be} are computed on the assumption $\Gamma\sim\Gamma_{\alpha_0}$.

It is interesting to note that of the four most prominent and clearly established levels three appear in the exact energy spacings associated with a rotational band structure (cf. Fig. 14). The interpolated position of the 0^+ level of the band at $E_{\alpha\ in}=12.85$ MeV, although not definitely established, is also not incompatible with the general trends indicated by the angular distributions.

It is difficult to tell whether this feature of the distribution of excitation energies is more than a remarkable coincidence. It is somewhat disturbing from the point of view of this interpretation that the widths of these levels do not exhibit any clear and regular pattern. In particular it is difficult to understand the extremely narrow width of the 4^+ level.

The relatively small width of the 6^+ may be due to the fact that this level is well below the classical limit for $L=6$.

Assuming a true rotational band structure for these levels the moment of inertia $\mathcal{J}$ defined by

$$E_J - E_0 = \frac{h^2}{2\mathcal{J}} J(J+1)$$

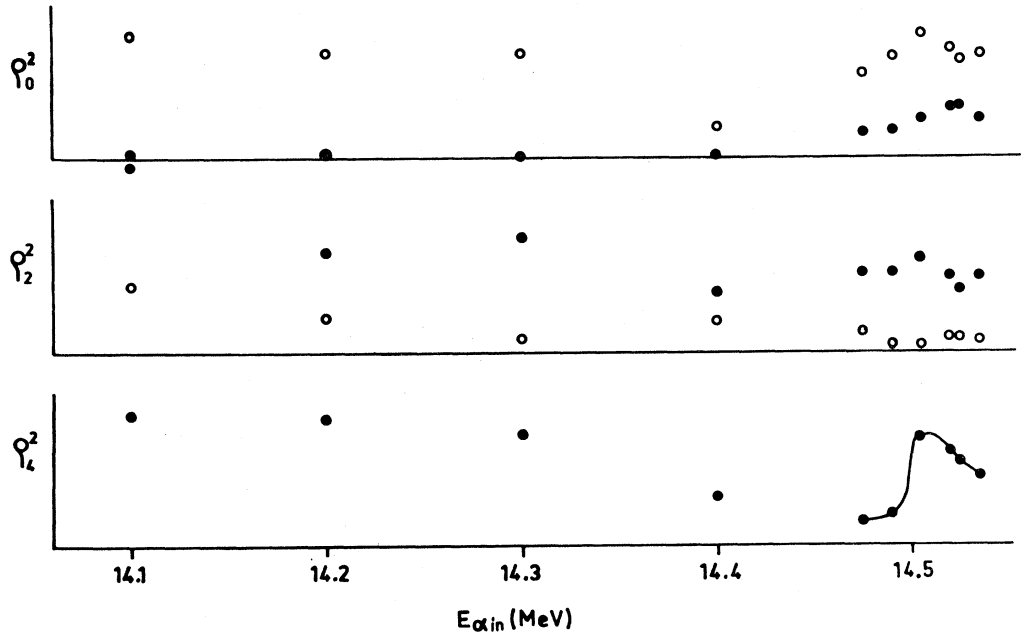

FIG. 13. The parameters ρ_0, ρ_2, and ρ_4 in the neighborhood of $E_{\alpha\ in}=14.50$ MeV. For ρ_0 and ρ_2 the two possible solutions are shown.

TABLE II. Properties of identified resonances. Even-parity resonances observed in $C^{12}(\alpha,\alpha)C^{12}$ in this region[a] are also shown for comparison.

$C^{12}+\alpha \rightarrow Be^8+Be^8$						$C^{12}+\alpha \rightarrow C^{12}+\alpha$			
$E_{\alpha\ \text{in}}$ (MeV)	$E^*(O^{16})$ (MeV)	J^π	Γ (keV)	σ^{tot} (mb)	ΓBe^8 (keV)	$E_{\alpha\ \text{in}}$ (MeV)	E^* (MeV)	J^π	Γ (keV)
13.05	16.95	2^+	370	7	6	12.9	16.8	(4^+)	525
13.35	17.15	2^+	260	11	7	13.3	17.1	$(1^-,2^+,0^+)$	110
						13.9	17.55	(4^+)	225
(14.1	17.7	$0^+,2^+$)							
(14.2	17.8	4^+)							
14.52	18.05	4^+	20	16	0.5	14.49	18.01	(4^+)	45
(15.2	18.6	$0^+,2^+$)							
(15.6	18.9	4^+)							
16.25	19.35	6^+	70	10	0.8	15.96	19.10	$(2^+,4^+)$	55
						16.30	19.35	$(4^+,0^+)$	30

[a] Reference 1.

is found to have the value

$$\mathcal{J}=21M(O^{16})(F)^2=3M(O^{16})R(O^{16})^2,$$

where $M(O^{16})$ is the mass of O^{16} and $R(O^{16})$ the radius, taken as 2.64 F.

This is a rather large moment of inertia, about four times the moments of inertia of the bands with band heads at 6.05 and 11.26 MeV,[1] and it implies a very extended structure of the O^{16} nucleus in these states. The only conceivable structure with such a moment of inertia is of four α's laid out in a string and rotating rigidly. The distance between centers of adjacent α's in this configuration is found to be 4.1 F, close to the diameter of the α particle. A similar structure has been suggested by Morinaga[6] for a rotational band in Mg^{24}.

ACKNOWLEDGMENTS

Part of this work was carried out at the Max Planck Institut fur Kernphysik in Heidelberg and we would like to express our most sincere appreciation and gratitude for the hospitality and help extended to us by the laboratory in general and most particularly to Professor Gentner, Dr. Bock, and Dr. Zimmerer.

[6] H. Morinaga, Phys. Rev. **101**, 254 (1956).

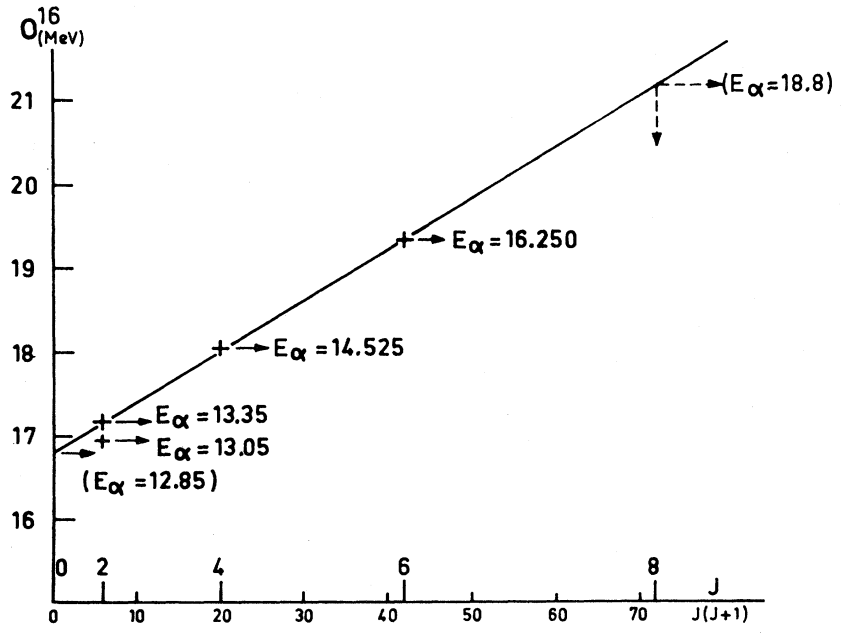

FIG. 14. The energies of the four established resonances on an $J(J+1)$ scale exhibiting a possible rotational-band structure of some of these levels.

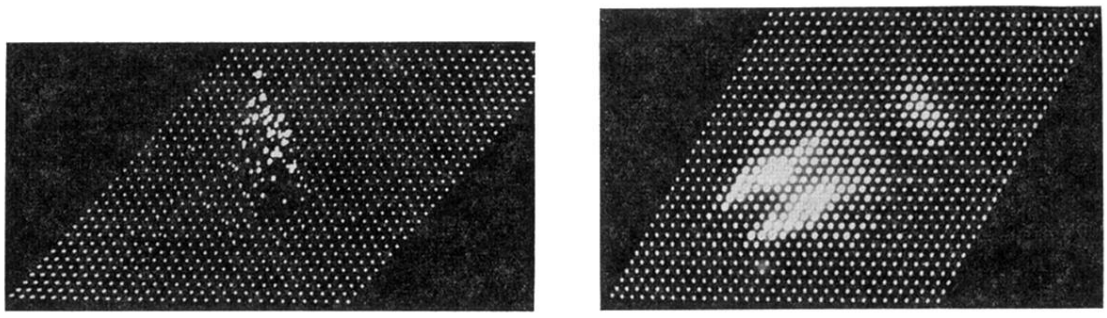

(a) (b)

FIG. 7. Two-dimensional spectra of the energies of the two α's. (a) A typical large-angle spectrum is shown in a "three-dimensional" display. Virtually all counts registered in this case correspond to $O^{16} \rightarrow Be^8 + Be^8$ decays. (b) A typical "small-angle" spectrum shown in an intensity-modulation display. The α pairs from $Be^8 + Be^8$ decays appear in this spectrum as the head of the little man.